



Investigation of average optical density and degree of liquids saturation in sand by image analysis method

Sitthiphat Eua-Apiwatch* and Siam Yimsiri

Department of Civil Engineering, Burapha University, Chonburi 20131, Thailand.

Received April 2016
Accepted June 2016

Abstract

This research aims to apply an image analysis technique to investigate relationships between liquid saturations and Average Optical Densities (AODs) of four different porous media (i.e., Ottawa#3820, Ottawa#3821, Toyoura, and Chonburi sands). Water and diesel are used as liquids. Twenty tested samples, including 10 samples of air-water two-phase system and 10 samples of air-diesel two-phase system with variations of diesel and water saturations, are prepared for each porous medium. All samples are compacted into cylindrical containers then photos of each sample are taken by two digital cameras fitted with different band-pass filters. The photos are analyzed by an in-house program to obtain average optical densities for each spectral band. Relationships between AODs and liquid saturations are analyzed for each porous media. The results indicate that AODs are linearly proportion to degree of water and diesel saturations for all porous media in both spectral bands except Chonburi sand. The reason is due to the fact that Chonburi sand has a very rough surface which can absorb water and other liquids more than other media.

Keywords: LANPLs, Diesel, Saturation, Image analysis method

1. Introduction

Diesel fuel and gasoline leakage from underground storage tank (UST) is one of the most common subsurface contamination problems. Petroleum hydrocarbons do not readily mix with water and are known as Non-Aqueous Phase Liquids (NAPLs) which can be classified into two types, i.e. denser than water (Dense Non-Aqueous Phase Liquids, DNAPLs) and lighter than water (Light Non-Aqueous Phase Liquids, LNAPLs). Understanding the distribution of NAPLs in the subsurface is important for cost-effective remediation strategies of contaminated aquifers. In laboratory investigation, measurement of NAPLs saturation is the most difficult and important task in acquiring precise data [1]. Most image techniques used photon-attenuation, such as gamma ray [2] and X-ray techniques [3] to obtain NAPLs saturation. Multispectral Image Analysis Method (MIAM) has been developed by Kechavarzi et al. [4] as an alternative tool for measuring saturation distributions of NAPLs, air, and water in laboratory experiments under dynamic condition. Kechavarzi et al. [4] successfully established linear relationships between NAPL (Soltrol 220) saturation, water saturation, and optical density of silica sand by using narrow spectral band-pass filter (10 nm large and centered at 500, 760, and 970nm) installed in digital near-infrared cameras.

This research aims to study saturation-optical density relationships in four different sand, i.e. Ottawa#3820, Ottawa#3821, Toyoura, and Chonburi sands. Diesel is

selected as a NAPL and two Nikon D90 digital cameras with 640 and 450 nm band-pass filters are used to capture reflected light intensity within each spectral band. An image analysis technique following Flores et al. [5] is used to obtain NAPL, air, and water saturations. Two-phase (air-water and air-diesel) relationships are established for all porous media.

2. Materials and methods

2.1 Multispectral image analysis method

Multispectral Image Analysis Method has been proposed by Kechavarzi et al. [4] and provides a non-destructive and non-intrusive tool to measure degree of liquids and air saturations in both two-phase and three-phase system under dynamic condition. It provided a relationship between Average Optical Densities (AOD) and degree of liquid saturations in sand. The Optical density (D_r) is defined in term of reflectance as shown in Eq. (1).

$$D_r = -\log\left(\frac{I_r}{I^0}\right) \quad (1)$$

where I is the intensity of the reflected light from interested object and I^0 is the intensity of the reflected light from an ideal white surface, respectively.

The quantity of liquid presented in the system can be captured by digital cameras fitted with band-pass filters. From digital images, AOD (D_i) can be defined in term of reflected light intensities as shown in Eq. (2).

*Corresponding author. Tel.: +6681 451 4387
Email address: sitthiphat@buu.ac.th
doi: 10.14456/kkuenj.2016.44

$$D_i = \frac{1}{N} \sum_{j=1}^N d_{ji} = \frac{1}{N} \sum_{j=1}^N \left[-\log_{10} \left(\frac{I_{ji}^r}{I_{ji}^0} \right) \right] \quad (2)$$

where N is the number of pixels in the interested area and, for a given spectral band i , d_{ji} is the optical density of each pixel, I_{ji}^r is the reflected light intensity from each pixel, and I_{ji}^0 is the reflected light intensity from ideal white surface.

In two-phase (air-water and air-diesel) system only one camera fitted with band-pass filter (wavelengths $\lambda = i$) is required. Liquid saturation (S) can be obtained from following equation.

$$D_i = aS + b \quad (3)$$

2.2 Material, Equipment and method

2.2.1 Material

Ottawa#3820, Ottawa#3821, Toyoura, and Chonburi sands are used in this study. Basic properties of these sands are presented in Table 1. Figure 1 presents X-ray diffraction technique (XRD) diagrams of all sands. The results show that a dominant mineral of all porous media is quartz. Albite is found in both Chonburi and Toyoura sands. Microcline is found only in Chonburi sand and Orthoclase is found only in Toyoura sand. Scanning Electron Microscopy (SEM) is conducted for all porous media to investigate morphological appearances at surface of sands. Obtained SEM micrographs are shown in Figure 2. Red dyed diesel by Red Sudan III (1:10000 by weight) is selected as LNAPL and blue dyed water by Brilliant Blue FCF (1:10000 by weight) is used in this study.

2.2.2 Equipment

Two Nikon D90 digital cameras each fitted with a band-pass filter (450 nm and 640 nm) are used to capture images. White balance, shutter speed, and aperture of both cameras are kept constant. Two computers are used in this experiment and each computer are connected to digital camera via USB cable to remotely control digital cameras by Nikon Camera control Pro 2 program. X-Rite Gretagmacbeth ColorChecker® white balance card is located close to the samples for white and black color reference. 30 W LED floodlights are applied in this experiment to lighten the sand samples. Equipment installation is shown in Figure 3.

2.2.3 Method

Known amounts of water and sand are mixed to produce 10 samples with a constant dry unit weight of sand with variation of water saturations. The samples are packed in 25 cm³ cylindrical shape container ($h = 20$ mm, $d = 40$ mm). Reflected light intensity of each sample are captured by both cameras which are located approximately 1.5 m away from the samples. To prevent evaporation of water, humidity and room temperature during test are kept constant at 70% and 20 °C, respectively. Diesel and sand are mixed with variation of diesel saturation to produce another 10 samples by similar procedures. Photos of all samples are recorded in NEF format and ViewNX 1.5.0 software is used to export all photos to TIFF format after that TIFF images are analyzed by MATLAB release 2007a following the methods of Flores et al. [5]. Image analysis procedure are presented in Figure 4.

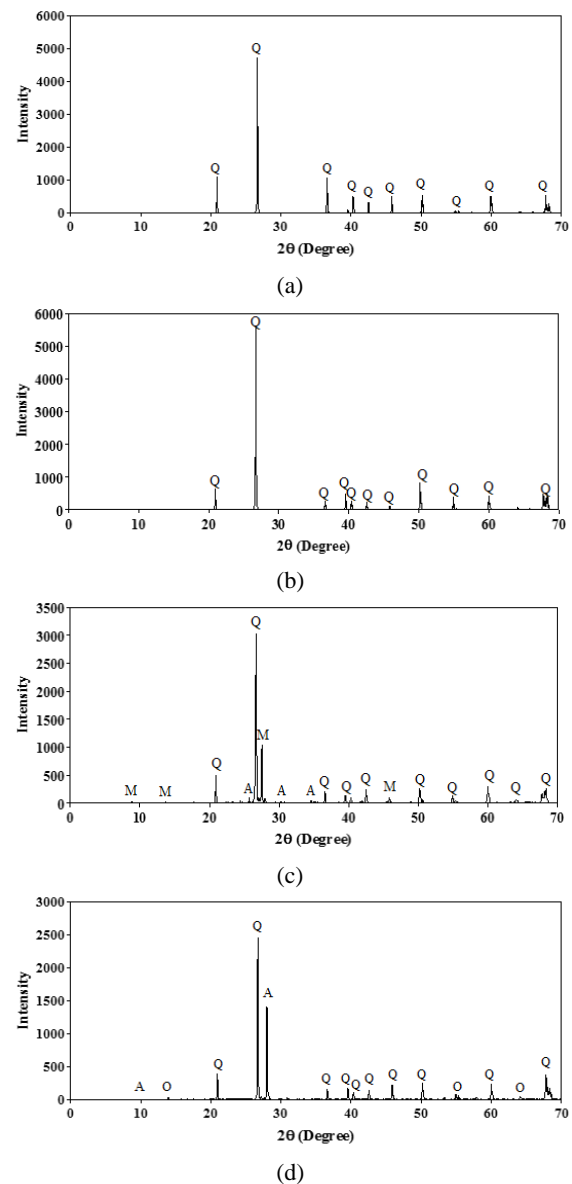
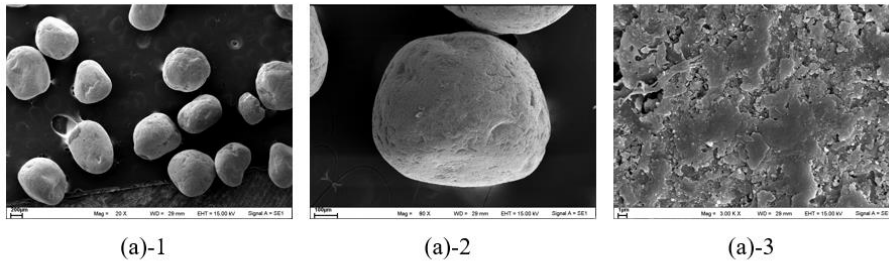


Figure 1 XRD diagram (a) Ottawa#3820 sand (b) Ottawa#3821 sand (c) Chonburi sand and (d) Toyoura sand. Peaks are due to Quartz (Q) (SiO₂), Microcline (M) (KAlSi₃O₈), Albite (A) (NaCa(SiAl)₄O₈ and Orthoclase (O) (KAlSi₃O₈)

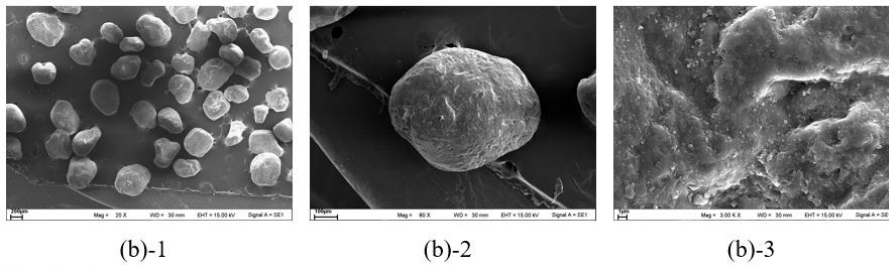
3. Results

AOD and water saturation relationships in different porous media for $\lambda = 450$ and 640 nm are presented in Figures 5 and 6, respectively. Image analysis results show that AODs in both wavelengths are linearly proportion to water saturations in each image for all porous media except Chonburi sand. The average optical density at wavelength $\lambda = 450$ nm of Chonburi sand is linearly independent with degree of water saturation and the coefficient of determination (R^2) in Table 2 shows the lowest value when compared to others porous media. At 640 nm wavelength, the coefficient of determination (R^2) is much better than at 450 nm wavelength indicating that the air-water two-phase system by image analysis method at 640 nm band-pass filter is more suitable than at 450 nm band-pass filter.

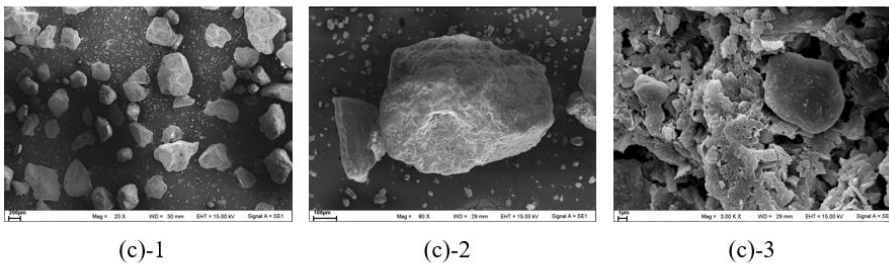
Ottawa#3820 sand



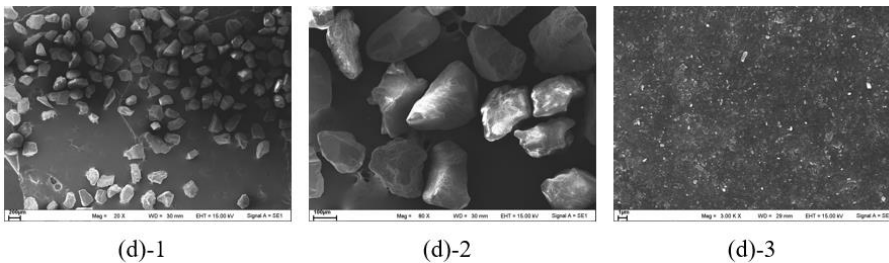
Ottawa# 3821 sand



Chonburi sand



Toyoura sand

**Figure 2** SEM micrographs of tested sand**Table 1** Basic properties of sand

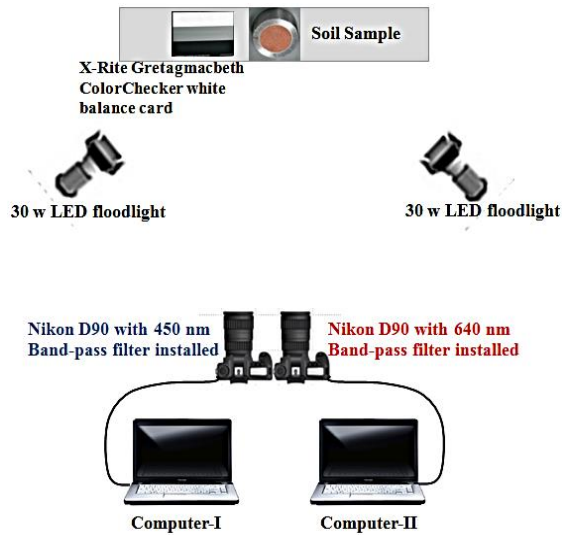
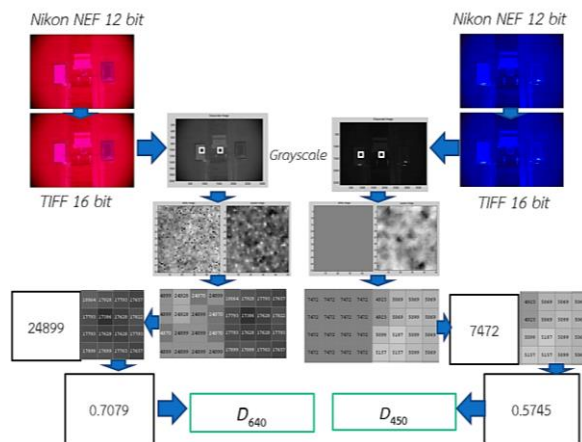
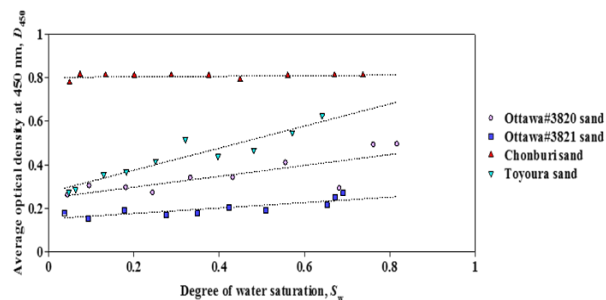
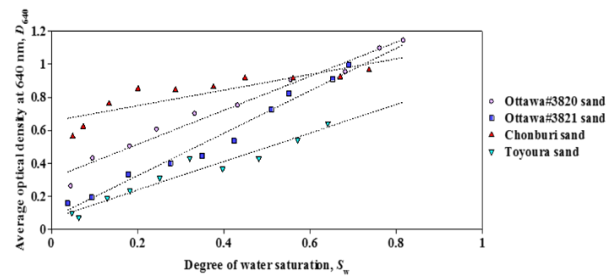
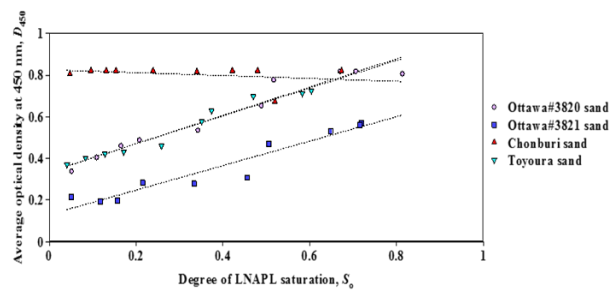
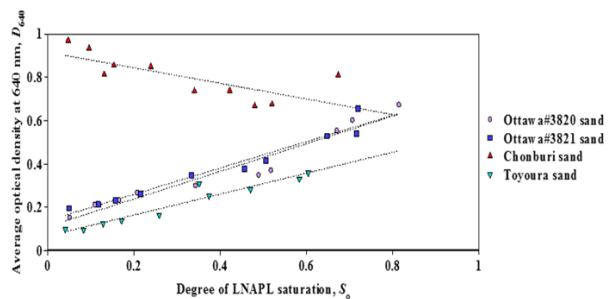
Properties	Ottawa#3820	Ottawa#3821	Chonburi	Toyoura
Particle density, ρ_s (g/cm ³)	2.64	2.63	2.66	2.61
Uniformity coefficient, C_u	1.47	1.56	2.68	1.51
Mean grain size (D_{50}), mm	0.643	0.422	0.397	0.224
Soil permeability, k (cm/s)	2.02×10^{-2}	1.80×10^{-2}	3.69×10^{-2}	2.01×10^{-3}
Average Porosity	0.375 ± 0.012	0.384 ± 0.016	0.426 ± 0.020	0.445 ± 0.016
USCS	SP	SP	SP	SP
LOI (%)	0.38	0.13	1.26	0.50

Table 2 AOD and water saturation relationships

Porous Media	D_{450}	R^2	D_{640}	R^2
Ottawa#3820 sand	$0.250 S_w + 0.248$	0.65	$1.029 S_w + 0.309$	0.98
Ottawa#3821 sand	$0.125 S_w + 0.152$	0.69	$1.284 S_w + 0.068$	0.98
Chonburi sand	$0.013 S_w + 0.802$	0.08	$0.472 S_w + 0.654$	0.75
Toyoura sand	$0.509 S_w + 0.273$	0.89	$0.862 S_w + 0.066$	0.95

Table 3 AOD and diesel saturation relationships

Porous Media	D_{450}	R^2	D_{640}	R^2
Ottawa#3820 sand	$0.669 S_o + 0.336$	0.94	$0.638 S_o + 0.111$	0.94
Ottawa#3821 sand	$0.588 S_o + 0.130$	0.92	$0.608 S_o + 0.138$	0.95
Chonburi sand	$-0.069 S_o + 0.825$	0.10	$-0.360 S_o + 0.916$	0.55
Toyoura sand	$0.680 S_o + 0.335$	0.96	$0.484 S_o + 0.068$	0.93

**Figure 3** Experimental set up**Figure 4** Image analysis procedure**Figure 5** AOD and water saturation relationships in different porous media for $\lambda = 450$ nm.**Figure 6** AOD and water saturation relationships in different porous media for $\lambda = 640$ nm.**Figure 7** AOD and diesel saturation relationships in different porous media for $\lambda = 450$ nm.**Figure 8** AOD and diesel saturation relationships in different porous media for $\lambda = 640$ nm.

In all porous media AOD and diesel saturation, have linear relationships except Chonburi sand as shown in Figures 7 and 8. AOD at 450 and 640nm of Chonburi sand have inverse relationships with degree of diesel saturation as presented in Table 3.

4. Discussion

AOD at both spectral bands of Chonburi sand exhibit inversely linear relationships with water and diesel saturations. SEM images (Figure 2c) show that the surface morphology of Chonburi sand is significantly different from other sands. The size distribution of Chonburi sand is large. Moreover, at high magnification, very rough particle surface is observed, which means that Chonburi sand may be able to absorb water and other liquids more than other media. These

observations are supported by the basic properties shown in Table 1, especially the highest hydraulic conductivity of Chonburi sand. In fact, at the time that the Chonburi-sand samples are prepared, liquids can be absorbed into the sand particles. SEM results and unsatisfactory coefficient of determination (R^2) obtained from Chonburi sand confirm that the optical technique, such as Multispectral Image Analysis Method, is not suitable for this kind of sand.

5. Conclusions

AOD, water saturation, and diesel saturation relationships are investigated for four different sands and it is experimentally found that linear relationships between AOD, degree of water saturation, and degree of diesel saturation are existed in all sands, except Chonburi sand because liquids can be absorbed into the surface of Chonburi sand particle. Therefore, the Optical technique, such as Multispectral Image Analysis Method, may be suitable for the investigation of NAPLs behavior in various kinds of media, except the media that can absorb the liquids, such as for the case of Chonburi sand, which is firstly found in this research.

6. Acknowledgements

This work was financially supported by the Research Grant of Burapha University through National Research Council of Thailand (Grant No. 168/2559)

7. References

- [1] Kamaruddin SA, Sulaiman WNA, Rahman NA, Zakaria MP, Mustaffar M, Sa'ari R. A review of Laboratory and Numerical Simulations of Hydrocarbons Migration in Subsurface Environments. *Journal of Environmental Science and Technology* 2011;4(3):191-214.
- [2] Ferrand LA, Milly PCD, Pinder GF. Experimental Determination of Three-Fluid Saturation Profiles in Porous media. *Journal of Contaminant Hydrology* 1989;4:373-395.
- [3] Tuck DM, Bierck BR, Jaffe PR. Synchrotron radiation measurement of multiphase fluid saturations in porous media: Experimental technique and error analysis. *Journal of Contaminant Hydrology* 1998;31(3-4):231-256.
- [4] Kechavarzi C, Soga K, Wiart P. Multispectral Image Analysis Method to Determine Dynamic Fluid Saturation Distribution in Two-Dimensional Three-Fluid Phase Flow Laboratory Experiments. *Journal of Contaminant Hydrology* 2000;46:265-293.
- [5] Flores G, Katsumi T, Inui T, Kamon M. A simplified image analysis method to study LNAPLs migration in porous media. *Soil and Foundations* 2011;51:835-847.